Title
METALLOGRAPHY OF BAINITIC TRANSFORMATION IN SILICON CONTAINING STEELS

Author
Huang, D-H.

Publication Date
1977-08-01

Submitted to Metallurgical Transactions

LBL-4519
Preprint

METALLOGRAPHY OF BAINITIC TRANSFORMATION IN SILICON CONTAINING STEELS

Der-hung Huang and Gareth Thomas

August 1977

Prepared for the U. S. Energy Research and Development Administration under Contract W-7405-ENG-48

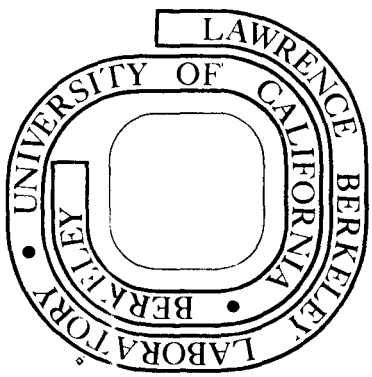

DISCLAIMER

LBL-4519

METALLOGRAPHY OF BAINITIC TRANSFORMATION IN SILICON CONTAINING STEELS

Der-hung Huang and Gareth Thomas

Department of Materials Science and Engineering, College of Engineering and Materials and Molecular Research Division, Lawrence Berkeley Laboratory, University of California, Berkeley, California 94720.

ABSTRACT

The formation of carbide in lower bainite was studied in two silicon containing carbon steels by transmission electron microscopy and diffraction techniques. Epsilon carbide was identified in the low temperature isothermally transformed bainite structure. The crystallographic relationship between epsilon carbide and bainitic ferrite was found to follow the Jack orientation relationship, viz., $(0001)\varepsilon||(011)\alpha$, $(10\bar{1}1)\varepsilon||(101)\alpha$. The cementite observed in lower bainite was in the shape of small platelets and obeyed the Isaichev orientation relationship with the bainitic ferrite, viz., $(010)c||(1\bar{1}1)\alpha$, $(103)c||(011)\alpha$. Direct evidence showing the sequence of carbide formation from austenite in bainite has also been obtained. Based on the observations and all the crystallographical features, it is strongly suggested that in silicon containing steels the bainitic carbide precipitated directly from austenite instead of from ferrite at the austenite/ferrite interface as has been proposed by Kinsman and Aaronson (Reference 1). The uniformity of the carbide distribution is thus envisaged to be the outcome of precipation at the austenite-ferrite interphase boundary.

I. INTRODUCTION

The term bainite, so named in honor of E. C. Bain, refers to the microstructural constituent formed in steels when austenite decomposes at temperatures above that for martensitic formation but below that for pearlite through either isothermal transformation or continuous cooling. The morphology of bainite changes gradually with reaction temperature, so no pronounced structural changes are observed over any small temperature range. Although the microstructure may assume a variety of forms, two major variants of bainite morphology, namely upper and lower bainite, are observed in steels transformed in different ranges of temperature[2-4].

The transformation mechanism of bainite has been a topic of discussion ever since the structure was first recognized. The problem is complicated in view of the fact that the bainite reaction often exhibits features characteristic of two basic classes of transformation in iron alloys, the diffusion controlled and the martensitic type. As pointed out in a recent debate on bainite[1], both the nature of carbides and whether the carbides in bainite precipitated from supersaturated ferrite or from austenite is of fundamental significance to the bainite reaction mechanism. It is generally accepted that cementite constitutes the carbide phase in upper bainite. Although cementite is likewise frequently observed in lower bainite, the exact carbide precipitation process is still uncertain. It has been reported that epsilon carbide is the first carbide formed in low temperature bainite which is subsequently replaced by cementite on further transformation[5-7]. These reports were based either on conclusions drawn indirectly from physical measurements or from direct electron microscopy observations[7]. Unfortunately, it has not always been possible to determine unambiguously the nature of the carbides present because of competing factors and their complex structures. In view of the lack of

totally definitive evidence for the identification of epsilon carbide in lower bainite in the literature, it was part of the purpose of the current investigation to provide such information, and to study the relevant crystallographic relationships.

Previous crystallographic studies of the orientation relationships between bainitic carbide and ferrite have suggested that these carbides precipitate from austenite in upper bainite and from ferrite in lower bainite[3,8]. These results are consistent with other evidence at high temperature and have generally been accepted. In the lower temperature range, however, there is still no universal agreement on the formation mechanism. One school of thought holds the view that lower bainite forms by a shear mechanism similar to that of martensite and the transformation is completed either by a subsequent tempering process resembling that of auto-tempering in martensitic steels or by a relaxation process[8]. This concept requires carbide precipitation from ferrite. It is supported by the evidence that the typical Bagaryatskii[9] ferrite/cementite orientation relationship occurring in martensite[10] was also found to exist between ferrite and cementite in lower bainite[3,8]. On the other hand, based on the calculated average carbon content of the retained austenite associated with partial transformation to bainite from x-ray diffraction data, it was concluded that bainitic carbide is more likely to precipitate directly from austenite[1]. Therefore, the origin of the carbide in lower bainite remains to be elucidated for verification of the transformation mechanism. Thus in the present study, the use of thin foil transmission electron microscopy and diffraction has been utilized to re-examine the morphological and crystallographical

features of cementite and ferrite in lower bainite, in order to try to provide experimental verification.

II. EXPERIMENTAL PROCEDURE

A. Materials and Heat Treatment

The chemical composition of the alloys under investigation are given in Table I along with their M_s temperatures which were determined by dilatometric measurements. The steels will be referred to by their designations as given in Table I. Note that the nominal composition is indicated by the alloy designation: the first digit represents nominal wt.% of the silicon content, the last two digits represent wt.% of carbon. Alloy 2S40 was vacuum melted and cast as a twenty-five pound ingot. After hot rolling, homogenization at 1300°C was done for several days. The details of heat treatment and the corresponding TTT diagram have been described in reference 11 which were followed to ensure that proper bainitic treatments were achieved.

The particular composition of the alloy 2S54 selected provided an opportunity to compare the results with those of Oblak and Hehemann[7] on the morphology and crystallography of the bainite transformation. Alloy 2S54 was vacuum induction melted in this laboratory using high purity material and poured in a fast chilled copper mold as a 1.8-kg. (4-lb.) ingot.

All materials were sandblasted to remove any surface oxide. They were subsequently homogenized at 1100°C for three days and furnace cooled. A simple low-cost but successful technique was employed to prevent decarburization during homogenization. The as-received or as-cast materials were wrapped in stainless steel envelopes then sealed inside an Inconel

tube filled with cast iron chips and a small amount of active charcoal. The cast iron chips provided enough carbon potential inside the Inconel tube during homogenization annealing so as to minimize any decarburization of the heat-treated material. Alloy 2S54 and 2S40 were then hot rolled to strips of 0.1 cm (0.040 in.) thickness, with intermediate surface grinding employed to remove any scale.

Coupons of 2.54 cm by 3.81 cm (1 in. by 1-1/2 in.) were cut from these strips, austenitized at 900°C for 1-1/2 hr. in a dynamic argon atomosphere, and then quenched directly into a neutral salt bath. Isothermal transformation was then accomplished at a predetermined temperature above M_s for a certain time. Carbon analyses before and after heat treatment showed no significant decarburization.

B. Electron Microscopy

Thin foils for transmission electron microscopy were prepared from the heat treated 0.1 cm (0.040 in.) thick specimens, by first mechanical grinding, followed by chemical thinning and finally electropolishing in a chromic-acetic acid bath. Foils were examined in a Seimens Elemiskop I A microscope, operated at 100 kV in both imaging and diffraction modes. For the identification of epsilon carbide, selected area diffraction patterns were indexed with the aid of tables of d-spacings and angles between crystallographic planes calculated from a general computer program which has been compiled for non-cubic crystal systems. The imput data were a = 2.735Å and c = 4.339Å, which yield a c/a ratio of 1.586 as determined by Jack[12].

III. RESULTS AND DISCUSSION

A. Isothermal Transformation at 275°C

Thin foils suitable for transmission electron microscopy were made from isothermally transformed lower bainite of steel 2S54. Although the precipitates were often very small and gave imcomplete diffraction patterns, the presence of epsilon carbide in lower bainite was detected by employing careful selected area diffraction and dark field imaging techniques.

Figure 1(a) shows the structure of lower bainite of the steel 2S54 after being isothermally transformed at 275°C for 17 hrs. A high density of carbide precipitates is distributed uniformly throughout the bainitic ferrite matrix. These carbides form as thin platelets or laths varying in size from 60 to 200Å wide and 700 to 4000Å long. The corresponding selected area diffraction pattern is shown in Fig. 1(b) together with its indexing. From this and many other photographs which give a variety of orientations of the ferrite and carbide with respect to the incident electron beam, it has been possible to determine the orientation relationship between the two phases. In Fig. 1, the matrix has the $[011]_{\alpha}$ zone orientation and the carbide is analyzed as epsilon carbide with $[0001]_{\varepsilon} \| [011]_{\alpha}$. It is clearly seen that the volume fraction of carbide is very large and the carbide/ferrite interface is rather ragged suggesting that the interface is partially or non-coherent and contains structural dislocations. In addition to the identification of epsilon carbide in lower bainite, the orientation relationships between epsilon carbide and bainitic ferrite may be obtained directly by plotting the orientations determined from the diffraction pattern, Fig. 1(b), on a stereographic projection as in Fig. 2. It is clearly seen that $(0001)_{\varepsilon}$ plane is

parallel with $(011)_\alpha$, and $(10\bar{1}1)_\varepsilon$ is only 1° from $(101)_\alpha$. This is practically the same as the Jack orientation relationship[12] which may be stated:

$$(0001)_\varepsilon \parallel (011)_\alpha$$
$$(10\bar{1}1)_\varepsilon \parallel (101)_\alpha$$

The one degree discrepancy between our result and that of Jack's is attributed to experimental errors.

Characteristic wavy epsilon carbide in better contrast is seen in one of the bainite grains in Fig. 3 which is another area of the same treated specimen as that in Fig. 1. The waviness of the carbide could be interpreted as simultaneous transformation, i.e. the epsilon carbide is deformed along with the ferrite when austenite decomposed. As indexed in the insert, the matrix gives a $[100]_\alpha$ diffraction pattern and the epsilon carbide is slightly tilted about five degrees from the $[11\bar{2}0]_\varepsilon$ zone, in agreement with the orientation relations shown in Fig. 2.

In order to provide unique identification of this microstructure of bainite, the tempered martensitic structure of this steel was also studied and is presented for comparison. Figure 4 shows an example of the structure obtained after water quenching a specimen of the same steel to martensite followed by tempering at 275°C for 17 hr. By comparing Figure 4 with Figures 1 and 3 it is seen that they are entirely different. For example, the structure in Fig. 4 is densely twinned, which is characteristic of high carbon martensite.[10] Analysis of the selected area diffraction pattern indicates that the orientation of the matrix and twin are $[\bar{1}\bar{3}1]$ and $[10\bar{1}]$ respectively. The twin

plane is $(\bar{1}21)_\alpha$. Both the bright field image and the selected area diffraction pattern demonstrated little evidence of carbide precipitation. The result is not surprising owing to the fact that silicon is well known, though not fully understood, for contributing tempering resistance when used as an alloying element in steel.[13,14] It is evident that lower bainite and tempered martensite are easily distinguishable in this alloy and consequently unique identification of lower bainite is established.

In summary, epsilon carbide has been unambiguously identified in lower bainite, with the orientation relationship between epsilon carbide and bainitic ferrite being that observed earlier by Jack[12] viz.,

$$(0001)_\varepsilon \,||\, (011)_\alpha$$
$$(10\bar{1}1)_\varepsilon \,||\, (101)_\alpha$$

It should be mentioned that a similar orientation relationship was also recently observed in lower bainite of a 300M steel.[15] However, the origin of the carbide in lower bainite as deduced from this latter research is quite different from ours, and will be discussed later.

The observed crystallographic orientation relationship between epsilon carbide and ferrite can be accounted for by formation of epsilon carbide in either supersaturated ferrite or austenite. They will be discussed as follows:

(i) Epsilon carbide formed in ferrite. In bainite, if epsilon carbide forms directly from supersaturated ferrite (though often assumed, this statement is unverified), there will be little difference between

bainite and martensite in the morphology of the precipitation process. The crystallographic analysis shows that the orientation relationship between epsilon carbide and bainitic ferrite is that suggested by Jack[12] observed in tempered martensite. This relationship also gives the following (Fig. 2):

$$(0001)_\varepsilon \;||\; (011)_\alpha$$
$$(10\bar{1}0)_\varepsilon \;||\; (\bar{2}11)_\alpha$$

The stereogram, Fig. 2, shows that in epsilon carbide and ferrite close-packed planes and directions are parallel in both structures. The lattice misfit between $(10\bar{1}0)_\varepsilon$ and $(2\bar{1}1)_\alpha$ planes is 1.2 percent which is the lowest mismatch between the two crystals. This orientation relationship for epsilon carbide in tempered martensite can be explained in terms of minimizing the surface energy at the relatively low formation temperature.[16-18]

(ii) Epsilon carbide formed in austenite. It is equally possible that epsilon carbide forms on the austenite side of the austenite/ferrite interface. Such a transformation can also give rise to the Jack relationship. Because of the close lattice matching between fcc austenite and epsilon carbide one could expect that the orientation relationship of the epsilon carbide in austenite to be the familiar one viz.,

$$(111)_\gamma \;||\; (0001)_\varepsilon$$
$$(1\bar{1}0)_\gamma \;||\; (1\bar{2}10)_\varepsilon$$

Unfortunately, it was not possible to retain enough austenite to verify this assumption. However, it has long been established that the K-S relationship[19] is obeyed between asutenite and bainitic ferrite formed at low temperature,[20] viz.,

$$(111)_\gamma \parallel (011)_\alpha$$
$$(1\bar{1}0)_\gamma \parallel (\bar{1}\bar{1}1)_\alpha$$

This leads to the ferrite/epsilon-carbide relationship of the Jack type[12] observed in the present research.

In a recent investigation,[21] a similar orientation relationship was observed when Ni_3Ti precipitated from austenite in a Fe/28Ni/2Ti alloy during ausaging. Upon transformation to martensite on subsequent cooling, the orientation relationship between Ni_3Ti and martensite retained that between the precipitates and the matrix before transformation, i.e., the austenite phase. The same orientation relationship has also been observed after isothermal decomposition of a molybdenum austenitic alloy where fibers of Mo_2C nucleated on the austenite side of the austenite/ferrite interface.[22,23] Both of these results indicate that the indirect evidence of the orientation relationship between epsilon carbide and austenite may be deduced from that observed between epsilon carbide and bainitic ferrite, the ferrite and austenite being themselves related by one of the K-S variants.

As will be shown and discussed in the later sections, the bainitic cementite in silicon steel was found to precipitate directly from austenite at the austenite/ferrite interface. This suggests that precipitation of epsilon carbide is also likely to occur in contact with austenite at the austenite/ferrite interface. This is contrary to the

conclusions of Lai,[15] who also observed the existence of the Jack orientation relationship in lower bainite but supported accordingly the view that epsilon carbide precipitated from supersaturated bainitic ferrite by analogy to tempered martensite. However, there are morphological differences and it is important to realize that two families of epsilon carbide in a characteristic criss-cross pattern are generally observed in tempered martensite, [16-18] while in lower bainite only one variant has ever been detected in previous electron metallographic studies [7,15] and in the present investigation, despite the fact that the same orientation relationship existed between the epsilon carbide and the ferrite component in both bainite and martensite. The present suggested model viz., that formation of either epsilon carbide or cementite occurs on the austenite side of the austenite/ferrite interface is also able to account for the unidirectional morphology of the carbide phase in bainite.

B. Isothermal Transformation at 315°C

As the isothermal transformation temperature was raised to 315°C a structure developed[7] which is unique to silicon containing steels. These structures do not exhibit the classical morphologies normally associated with bainite and an example is presented in Fig. 5 which shows the microstructure of bainite after 17 min. of transformation. S-shaped second phase particles are found to be distributed throughout the structure. As will be shown in the following, detailed analysis indicates that the specimen contains bainitic ferrite, cementite and austenite. The problem of uniquely identifying austenite and cementite in these structures is not trivial. Careful choice of the proper orientation is needed so that selection of well defined austenite and cementite diffraction spots can be done to obtain appropriate dark

field images. Such an example is given in Fig. 6. Fig. 6(a) represents the bright field image of the bainite structure obtained by isothermal transformation at 315°C for 24hr. Stringer shaped structures can be seen roughly along the long axis of the bainitic ferrite grain. The corresponding selected area diffraction pattern is shown in Fig. 6(b) and is indexed in Fig. 6(c). The analysis shows that the bainitic ferrite is in [111] orientation and austenite in [011], following the Kurdjumov-Sachs orientation relationship.[19] A third constituent is identified as cementite in the [010] Fe_3C zone. Dark field imaging of the $(1\bar{1}1)$ austenite diffraction spot, Fig. 6(d), reverses the contrast for the austenite which positively shows that the wide stringers mainly at the lath boundaries are untransformed austenite. Figure 6(e) is the dark field image using a $(\bar{2}01)$ cementite diffraction spot. A thin layer of cementite, as indicated by the arrow, is revealed in contact with the austenite. Thus the formation of bainitic carbide is seen to bear a definite relationship to the untransformed austenite. Further evidence of the above-mentioned morphology is presented in Fig. 7(a). The diffraction pattern and the analysis are the same as those for Fig. 6. The dark field micrograph, Fig. 7(b), using the $(\bar{1}1\bar{1})$ austenite diffraction spot clearly shows the distribution of untransformed austenite. Many of these austenitic areas follow lath boundaries and then bend into the matrix as indicated by the arrows. In some other areas similar microstructures are seen in which the lath boundaries are extensively "decorated". However, here untransformed austenite has been decomposed to a further extent than is shown in Fig. 6 and 7, and this can only be revealed by selective dark field

illumination. As indicated by the arrows in Fig. 8, when both the $(\bar{2}01)$ cementite and $(1\bar{1}\bar{1})$ austenite diffraction spots are imaged, the untransformed austenite appears to have stepped interfaces enveloping the growing front of ferrite.

It has been proposed by Aaronson et al.,[24,25] that the ferrite component in austenite develops by a ledge mechanism during isothermal transformation. This mechanism involves ferrite growth primarily by the formation and lateral movement of ledges through diffusional jumps across the edge of the ledge. The kink shaped carbides could be indicative of such ledges left by the movement of the asutenite/ ferrite interface. However, the details of ledges in bainite have not yet been resolved by transmission electron microscopy. A recent in-situ investigation of the bainite reaction by using high voltage electron microscopy indicated that no ledge was observed when a Fe/9.1Ni/0.51C alloy was isothermally transformed to bainite at 380°C,[26] but since this was not done in a controlled environment nor were high resolution techniques utilized, the validity of the experiment is open to question. Thus, more conclusive evidence is needed, requiring sophisticated electron microscopy studies on the detailed interface structures.

The untransformed austenite will eventually decompose into carbide and ferrite after prolonged holding. The structure of bainite after transformation at 315°C for a longer period, 168 hr, is shown in Fig. 9(a). There are no marked differences between this structure and that after transformation for shorter times, e.g., Figs. 5 to 8. However, no reflections corresponding to austenite were detected in the selected area diffraction pattern Fig. 9(b). As shown in the

analysis, Fig. 9(c), the cementite is in [1$\bar{2}\bar{2}$] orientation, with ferrite in [$\bar{1}$00] and [111]. Cementite particles are clearly delineated in the dark field image of a (201) cementite diffraction, Fig. 9(d). Thus the decomposition of the untransformed austenite into ferrite and cementite seems to be complete in this specimen. The above observations provide direct evidence for the transformation path of cementite in bainite. Similar decomposition of retained austenite has been observed in the tempering of martensite which results in cementite precipitation along the martensite boundaries in addition to the accompanying Widmanstatten carbide formation inside the martensite matrix.[27]

It should be emphasized that the bainite structures described above are more complex than those associated with conventionally described upper and lower bainite (e.g. ref. 3) and cannot be classified only according to the orientation and distribution of the cementite particles. The conventional classification is further complicated by the general rule (true or not) that the bainite morphology changes over a relatively narrow temperature range being described as upper bainite above 350°C and lower bainite below about 350°C (e.g. ref. 1,3). Moreover, whilst many published micrographs can be easily identified morphologically as portraying either upper or lower bainite, yet the bainite structure in an Fe/Cr/C alloy[8] has been concluded to be lower bainite despite the presence of elongated bainitic carbides which morphologically implies that the product may be upper bainite. Thus we believe it is best to describe the present microstructure simply as bainite in order to avoid possible confusion.

C. Suggested Sequence for Bainitic Transformation

From these observations, it can be postulated that at 315°C, the bainite in silicon steel probably forms in the following sequence. The bainitic ferrite which nucleates and grows from the austenite grain boundary is arrested in growth periodically as a result of solute (carbon) enrichment of the adjacent austenite. Cessation of growth due to carbon enrichment can only occur when the carbon content of the austenite in either the specimen as a whole, or in a small region totally enclosed by ferrite, attains that of the A_e3 curve or its metastable equilibrium extrapolation. Below the eutectoid range, growth can only resume if carbide precipitation occurs in the austenite. Due to the rapid diffusion of carbon in austenite away from the growing ferrite[28,29] and the low rate of nucleation of carbide in the presence of silicon, a layer of metastable austenite is retained along the austenite/ferrite grain boundaries.
Other ferrite units may form from this layer of austenite following the same sequence. Repetition of this discontinuous growth mode can give rise to the observed "bamboo shaped" bainitic structure. Meanwhile, carbides precipitate gradually from the untransformed austenite during isothermal holding thereby delineating the previous position of the austenite/ferrite interphase boundary. After prolonged isothermal holding the untransformed austenite will decompose completely resulting in the observed bainitic ferrite - cementite composite.

The advantage of using silicon in the steel is that it appears to retard austenite decomposition. Thus in non-silicon containing steels, the carbide probably precipites rapidly and the decomposition of untransformed austenite may be too fast for its existence to be detected.

A similar growth model has been proposed by Shackleton and Kelly[3] for bainite formed at a higher temperature range, i.e., 400-500°C. Their crystallographic data suggested that cementite and ferrite can nucleate independently in austenite although this was not detected in their transformation product. The present observations demonstrate that carbides may form from austenite even at a low temperature and the particular carbide morphology results from precipitation along the austenite/ferrite interface. Another growth model has also been suggested by Oblak and Hehemann[7] to describe microstructures similar (but not identical) to the ones reported here. They considered this type of bainite morphology to be due to rapidly growing substructural units which propagated to a limited size. Delayed precipitation of cementite from bainite permits substantial partitioning of carbon to the austenite trapped in between ferrite laths. Cementite may subsequently precipitate from this enriched austenite.

Although the above explanations are consistent with the observed microstructure, the current detected s-shaped carbides cannot be adequately explained by this mechanism alone. Further direct evidence is required to test this shear-model conclusively.

In summary, to account for the observed particular bainitic morphology, the current proposed sequence of bainite formation is not contradictory to any of the existing models as far as the origin of carbides is concerned.

D. Isothermal Transformation at 400°C

At this higher transformation temperature, the ferrite regions in the Si steel are in general coarser than those found after the lower temperature treatments. This is seen very clearly in Fig. 10 which shows the bright field and a cementite dark field image of the bainite of steel

2S40 isothermally transformed at 400°C for 7 hr. This structure is typical of lower bainite consisting of ferrite and unidirectional cementite platelets.

The shape of the cementite particles, although appearing to be lath-like in many cases, was confirmed to be platelets, by tilting and observing bainite in the direction nearly perpendicular to the cementite habit plane as shown in Fig. 11(a). In the selected area diffraction pattern, Fig. 11(b), the matrix and the cementite were indexed as $[\bar{1}\bar{1}0]_\alpha$ and $[10\bar{1}]_c$ orientations respectively [Fig. 11(c)]. The stereographic analysis of the diffraction pattern, Fig. 11(d), shows that the orientation relationship is close to, but not exactly, that of Bagaryatskii[10]:

$$(100)_c \,||\, (\bar{1}01)_\alpha$$
$$(010)_c \,||\, (1\bar{1}1)_\alpha$$
$$(001)_c \,||\, (121)_\alpha$$

This relationship is the same as that previously observed by other workers for bainite[3,8] and tempered martensite[10]. By close examination of the stereogram, it is seen that the cementite/ferrite orientation relationship deviates slightly from the of Bagaryatskii as observed before [3,8]. After numerous investigations on this alloy and in other steels e.g., Fe/12Ni/4Co/0.4C and Fe/3.14Mn/0.37C[30] it was found that this deviation is real and can be interpreted in an alternative way. Much better agreement can be obtained by the Isaichev orientation relationship[31] viz.,

$$(010)_c \,||\, (1\bar{1}1)_\alpha$$
$$(103)_c \,||\, (011)_\alpha$$

The same orientation relationship has also been observed earlier in a plain carbon steel by Ohmori[32]. It is seen that in the Isaichev orientation relationship, the ferrite lattice is rotated around the

$[1\bar{1}1]$ pole by about 4° with respect to the Bagaryatskii relationship. It appears that this small difference between the two lattice relationships is significant in the argument as to whether cementite forms in austenite or in ferrite. As mentioned before, cementite is related to bainitic ferrite by the Isaichev orientation relationship and the ferrite/austenite lattice relationship follows that of Kurdjumov-Sachs. The orientation correspondence of the three crystals, i.e., austenite, ferrite and cementite can be summarized in Fig. 12 after the proper cyrstallographic variants have been chosen. The relationship between the three structures can now be expressed uniquely as follows:

$$(100)_c \,||\, (5\bar{4}5)_\gamma \text{ 4.76° from } (101)_\alpha$$
$$(010)_c \,||\, (10\bar{1})_\gamma \,||\, (11\bar{1})_\alpha$$
$$(001)_c \,||\, (252)_\gamma \text{ 4.76° from } (\bar{1}21)_\alpha$$

It should be noted that the above relationships between bainitic carbide and austenite are those which are involved in the relevant variant of the Pitsch lattice relationship[33,34] which was obtained when cementite formed in austenite. This crystallographic analysis thus supports the theory that bainitic carbides form originally in austenite instead of in ferrite[1].

The perpetual dispute over the source of bainitic carbides warrants further discussion. It still remains to be answered as to why the carbide particles in lower bainite precipitate unidirectionally. Based on the observed morphology and crystallography of bainitic carbides, attention will be focused on the possibility whether cementite precipitates in ferrite or in austenite.

The fact that in lower bainite the carbides form with only one variant instead of in the Widmanstatten morphology has led various investigators to believe that it must be precipitating on some kind of planar inhomogeniety. Shackleton and Kelly[3] suggested that the bainitic ferrite that forms martensitically from austenite may be twinned and the cementite may subsequently precipitate on these twin boundaries, i.e. on the {112} ferrite planes. Although no internal twinning has ever been reported in lower bainite, it has been argued that during tempering the twins are removed by the precipitation of cementite. This explanation seems to be unlikely since internal twins are not easily removed by tempering martensite even at higher temperatures than that used for isothermal transformation to bainite. Secondly the habit plane of the bainitic carbides was recently found to deviate from the {112} ferrite planes both in this alloy and other alloy systems, e.g. Fe/Ni/Co/C[30] and is not close to {110} which is a twin plane in high carbon martensite[35]. Hence, the unidirectional morphology of bainitic carbide is not likely to be due to carbide precipitation on twins as in the case of martensite[10].

It has also been suggested that cementite precipitation might take place on stacking faults produced during martensitic transformation of supersaturated ferrite from austenite[36]. This is not convincing because stacking faults are rarely observed in body centered cubic structures and never in α-iron. The crystallographic observations on lower bainite in an Fe/7.9Cr/1.1C alloy by Srinivasan and Wayman[8] shows that the observed habit plane of bainite in this alloy is different from that of the martensite in the same alloy. They also found that internal twinning could not explain the observed habit plane and the austenite-ferrite orientation relationship. It was subsequently considered that cementite precipitation takes place in ferrite behind the advancing austenite/ferrite interface. However, the current crystallographic analysis, Fig. 12, has shown that bainitic carbide can be related directly to austenite by the Pitsch

orientation relationship[33,34] suggesting that cementite may originate from austenite. Nevertheless, this would not differ from that of the precipitation of proeutectoid cementite from austenite. Besides the unidirectional morphology of cementite cannot be accounted for if cementite precipitates in the bulk austenite.

Since it is almost certain that carbide particles form on some particular crystallographic planes, an alternative suggestion is that the cementite is formed on the austenite side of the austenite/ferrite interface, as has been also suggested by Ohmori[32] and can be inferred from Ref. 8. Both the ferrite/cementite and the austenite/cementite orientation relationships should be concomitantly satisfied in this case. As pointed out in the stereogram, Fig. 12, this lattice relationship is in fact achieved.

The above analysis considers bainitic carbide to form on the austenite side of the austenite/ferrite interface without inferring the mechanism by which bainitic ferrite is formed. The uniformity of the carbide distribution in lower bainite is thus envisaged to be the outcome of discontinuous precipitation of cementite at the moving austenite/ferrite interface boundary.

IV. SUMMARY AND CONCLUSIONS

Epsilon carbide has been unambiguously identified in the bainitic structure of an Fe/1.87Si/0.54C steel when isothermally transformed at 275°C. The orientation relationship between epsilon carbide and bainitic ferrite was found to follow that of the Jack relationship[12], viz., $(0001)_\varepsilon || (011)_\alpha$, $(10\bar{1}1)_\varepsilon || (101)_\alpha$. When transformed at 315°C, a layer of untransformed austenite was detected to exist along the boundary of the ferrite component of bainite, and bears the Kurdjumov-Sachs relationship[19]. Upon further isothermal holding, the austenite decomposed into cementite and ferrite resulting in the characteristic "bamboo shaped" bainitic

microstructure observed in silicon containing steels. Thus, the current experimental observations support the theory that the bainitic carbide precipitates directly from austenite instead of from ferrite[1]. It has been shown by thermodynamic calculations that the average mole fraction of carbon in enriched austenite increases with decreasing transformation temperature[1]. At low transformation temperature carbon enrichment in untransformed austenite is high which may result in the observed precipitation of epsilon carbide. At higher reaction temperatures cementite forms in untransformed austenite probably because the carbon content corresponding to the extrapolated A_e3 is less. The kinetics of precipitation also determine the nature of the carbide formed.

At 400°C, the transformation of an Fe/1.73Si/0.4C steel produces structure of cementite platelets embedded in bainitic ferrite. The Isaichev orientation relationship[31] was observed between cementite and ferrite instead of that of Bagaryatskii.[9] Together with the Kurdjumov-Sachs relationship[19] obeyed between bainitic ferrite and austenite, it is shown that the bainitic carbide can be related directly to the austenite. Thus the morphological examination and the crystallographic analysis of the orientation relationship between ferrite, cementite and austenite lead to the conclusion that in silicon containing steel the carbide particles form on the austenite side of the austenite/ferrite interface.

The observation of epsilon carbide and cementite in bainite with different morphologies when transformed at different temperatures indicates that carbide precipitation in the bainite reaction depends on the transformation temperature as well as the composition of the steel.

ACKNOWLEDGEMENTS

We should like to thank Professor H. I. Aaronson for many discussions and encouragement to proceed with this research especially in regard to the question of the origin of carbide precipitation. We are also grateful to Professors R. F. Hehemann and N. F. Kennon for careful reviews and helpful comments on the manuscript. This work was done under the auspices of the Energy Research and Development Administration through the Inorganic Materials Research Division of the Lawrence Berkeley Laboratory, University of California.

REFERENCES

1. R. F. Hehemann, K. R. Kinsman and H. I. Aaronson: Met. Trans., 1972, vol. 3, p. 1077.
2. Electron Microstructure of Bainite in Steel, Second Progress Report by Subcommittee XI of Committee E-4, ASTM Proc., 1952, vol. 52, p. 543.
3. D. N. Shackleton and P. M. Kelly: The Iron and Steel Institute, Special Report No. 93, 1965, p. 126; Acta Met., 1967, vol. 15, p. 979.
4. F. B. Pickering: Transformation and Hardenability in Steels, Climax Molybdenum Co., Ann Arbor, 1967, p. 109.
5. S. J. Matas and R. F. Hehemann: Trans. TMS-AIME, 1961, vol. 221, p. 179.
6. J. Deliry: Mem. Sci. Rev. Met., 1965, vol. 62, p. 527.
7. J. M. Oblak and R. F. Hehemann: Transformation and Hardenability in Steels, p. 15, Climax Molybdenum Co., Ann Arbor, 1967.
8. G. R. Srinivasan and C. M. Wayman: Acta Met., 1968, vol. 16, p. 609 and 621; Trans. TMS-AIME, 1968, vol. 242, p. 79.
9. Y. A. Bagaryatskii, Doklady Adademiia Nauk SSSR, 1950, vol. 73, p. 1161.
10. P. M. Kelly and J. Nutting Proc. Royal Soc., 1960, vol. A259, p. 45; JISI, 1961, vol. 197, p. 199.
11. H. I. Aaronson and H. A. Domian: Trans. TMS-AIME, 1966, vol. 236, p. 781.
12. K. H. Jack: JISI, 1951, vol. 169, p. 26.
13. W. S. Owen: Trans ASM, 1954, vol. 46, p. 812.
14. W. C. Leslie, R. L. Pickett, C. P. Stoble and G. Konovol: Trans. ASM, 1961, vol. 53, p.715.
15. G. Lai: Met. Trans A, 1975, vol. 6A, p. 1469.

16. E. Tekin and P. M. Kelly : Precipitation from Iron-Base Alloys, G. R. Speich and J. B. Clark, eds., p. 173, Gordon and Breach, New York, 1963.

17. M. G. H. Wells: Acta Met., 1964, vol. 12, p. 389

18. S. Murphy and J. A. Whiteman: Met. Trans., 1970, vol. 1, p. 843.

19. G. Kurdjumov and G. Sachs: Z. Physik, 1930, vol. 64, p. 325.

20. G. V. Smith and R. F. Mehl: Trans. AIME 1942, vol. 150, p. 211.

21. I-Lin Cheng and G. Thomas: Met. Trans., 1972, vol. 3, p. 503.

22. F. G. Berry, A. T. Davenport and R. W. K. Honeycombe: Inst. of Metals, Monograph No. 33, 1969, p. 288.

23. F. G. Berry and R. W. K. Honeycombe: Met. Trans., 1970, vol. 1, p. 3297.

24. H. I. Aaronson, C. Laird and K. R. Kinsman: Phase Transformations, ASM, p. 313.

25. K. R. Kinsman, E. Eichen and H. I. Aaronson: Met. Trans., 1971, vol. 2, p. 346.

26. M. Nemoto: High Voltage Electron Microscopy, P. Swann, L. Humphery and M. Goringe, Eds., p. 230, 1974.

27. J. A. McMahon and G. Thomas: Third International Conf. on the Strength of Metals and Alloys, Cambridge, England, 1973, p. 180, vol. 1 (Inst. of Metals, London).

28. L. Kaufman, S. V. Radcliffe and M. Cohen: Decomposition of Austenite by Diffusional Process, H. I. Aaronson and V. F. Zackay: Eds., p. 313, Interscience, N.Y., 1962.

29. G. R. Speich and M. Cohen: Trans. AIME, 1960, vol. 218, p. 1050.

30. D. Huang and G. Thomas: Unpublished research,University of California, Berkeley.

31. I. V. Isaichev: Zhur, Tekhn, Fiziki, 1947, vol. 17, p. 835.

32. Y. Ohmori: Trans. ISI, Japan, 1971, vol. 11, p. 95.

33. W. Pitsch: Acta Met., 1962, vol. 10, p. 897.

34. W. Pitsch, Arch. Eisenhutt Wess., 1963, vol. 34, p. 381 and 641.

35. M. Oka and C. M. Wayman, Trans. TMS-AIME, 1968, vol. 242, p. 337.

36. K. Shimizu, T. Ko and Z. Nishiyama, Trans. Japan Inst. of Metals, 1964, vol. 5, p. 225.

TABLE I

Chemical Composition of the Alloys (in wt%) with their M_S Temperatures

Designation	Composition	M_S Temperature
2S54	Fe-0.54C-1.87Si-0.79Mn-0.30Cr	250°C(482°F)
2S40*	Fe-0.40C-1.73Si	370°C(698°F)

* We are grateful to Dr. H. I. Aaronson for providing this alloy.

FIGURE CAPTIONS

Fig. 1 (a) Structure of bainite which was obtained in isothermally transformed steel 2S54 (Fe-1.87Si - 0.54C + 0.79Mn-0.3Cr) at 275°C for 17 hr; (b) the corresponding selected area diffraction pattern showing a $[0001]_{\varepsilon}$ zone parallel with a $[011]_{\alpha}$ zone.

Fig. 2. Stereographic projection, based on the orientations determined in Fig. 1, representing the orientation relationship between epsilon carbide and bainitic ferrite.

Fig. 3. Another area of the bainite formed in steel 2S54 at 275°C characteristic wavy epsilon carbide with size of 60 to 200Å in width and 700 to 4000Å in length are seen in a bainitic ferrite grain. The insert shows the selected area diffraction pattern where the foil orientation is [100] and the epsilon carbide is in approximate $[11\bar{2}0]$ orientation.

Fig. 4. Structure of martensite of steel 2S54 tempered at 275°C for 17 hr. (a) shows typical internally twinned martensite plate where no carbide was detected. It is distinctly different from the bainitic structure; (b) selected area diffraction pattern and indexed representation showing orientation of the matrix and twin are $[\bar{1}\bar{1}1]$ and $[10\bar{1}]$ respectively. Twin plane is $(\bar{1}21)$.

Fig. 5. Structure of bainite in steel 2S54 after isothermal transformation at 315°C for 17 minutes, showing unique "S-shaped" untransformed austenite and cementite.

Fig. 6. Structure of bainite in steel 2S54 after isothermal transformation at 315°C for 24 hrs. (a) bright field micrograph showing untransformed austenite and cementite embedded in dislocated

bainitic ferrite grain; (b) the corresponding selected area diffraction pattern;, (c) indexing of pattern, showing the ferrite, austenite and cementite in $[111]_{\alpha}$, $[011]_{\gamma}$ and $[010]_{Fe_3C}$ zones respectively. The Kurdjumov-Sachs orientation relationship is followed between bainitic ferrite and austenite; (d) the untransformed austenite reverses contrast in the dark field image using the $(1\bar{1}1)$ austenite reflection; (e) a very thin layer of cementite (pointed by arrow) in contact with austenite is seen clearly in the dark field image of the $(\bar{2}01)$ cementite reflection.

Fig. 6. Another region of bainite in steel 2S54 obtained by isothermal transformation at 315°C for 24 hrs; (a) bright field micrograph showing "S-shaped" untransformed austenite forms along the lath boundary and then bends into the ferrite lath, the selected area diffraction pattern is the same as in Fig. 6; (b) the unique shape of retained austenite is pointed out by arrows in the dark field image of the $(\bar{1}1\bar{1})_{\gamma}$ diffraction spot.

Fig. 8. Dark field micrograph showing another area of the bainite in steel 2S54 after transformed at 315°C for 24 hrs. Both the carbide and austenite are in bright contrast by imaging the $(\bar{2}01)$ cementite and $(1\bar{1}1)$ austenite diffraction spots. Ferrite appears to be enveloped by untransformed austenite.

Fig. 9. Bainite in steel 2S54 obtained by isothermal transformation at 315°C for 168 hrs; (a) bright field micrograph showing ferrite lath with cementite; (b) the corresponding selected area diffraction pattern; (c) indexed pattern showing ferrite in $[\bar{1}00]$ and [111] orientation and the cementite in $[1\bar{2}\bar{2}]$ zone, no austenite is

detected; (d) dark field illumination of a (201) cementite reflection showing carbides in bright contrast.

Fig. 10. Structure of typical lower bainite in steel 2S40 (Fe-1.73Si-0.4C) after isothermal transformation at 400°C for 7 hrs: (a) cementite particles embedded unidirectionally in bainitic ferrite. These carbides are in bright contrast in dark field as in (b).

Fig. 11. (a) Structure of bainite in steel 2S40 obtained by isothermal transformation at 400°C for 7 hrs. showing cementite platelet have precipitated; (b) the corresponding selected area diffraction pattern, which is indexed in (c), demonstrating the ferrite matrix in $[\bar{1}\bar{1}0]_\alpha$ zone and cementite in $[10\bar{1}]_{Fe_3C}$ (d) stereographic projection summarising the lattice relationship between cementite and bainitic ferrite; Isaichev orientation relationship, viz., $(010)_c||(1\bar{1}1)_\alpha$, $(103)_c||(011)_\alpha$.

Fig. 12. Stereographic projection summarizing the orientation relationship between austenite, cementite and ferrite where K-S relationship, is obeyed between ferrite and austenite viz., $(011)_\alpha||(111)_\gamma$, $(11\bar{1})_\alpha||(10\bar{1})_\gamma$ and $(\bar{2}1\bar{1})_\alpha||(\bar{1}2\bar{1})_\gamma$; and the Isaichev correspondence, viz., $(010)_c||(11\bar{1})_\alpha$ and $(103)_c||(011)_\alpha$ is observed between cementite and ferrite.

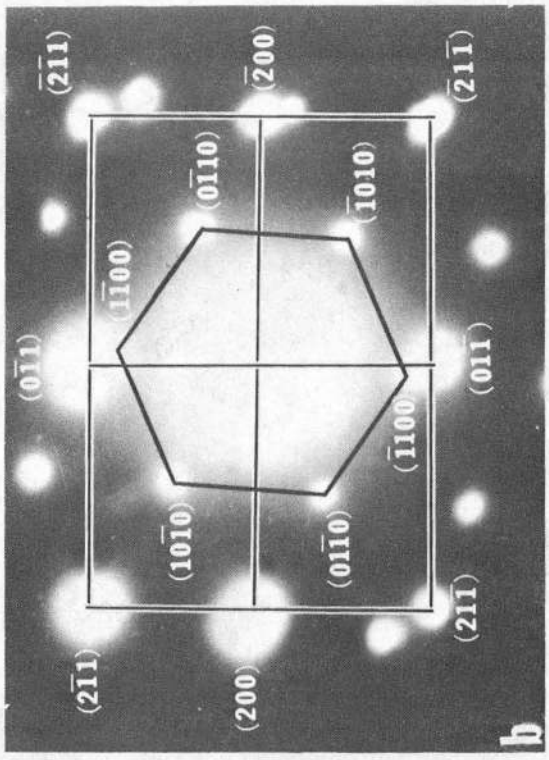

BAINITIC FERRITE ORIENTATION [011]
EPSILON CARBIDE ORIENTATION [0001]

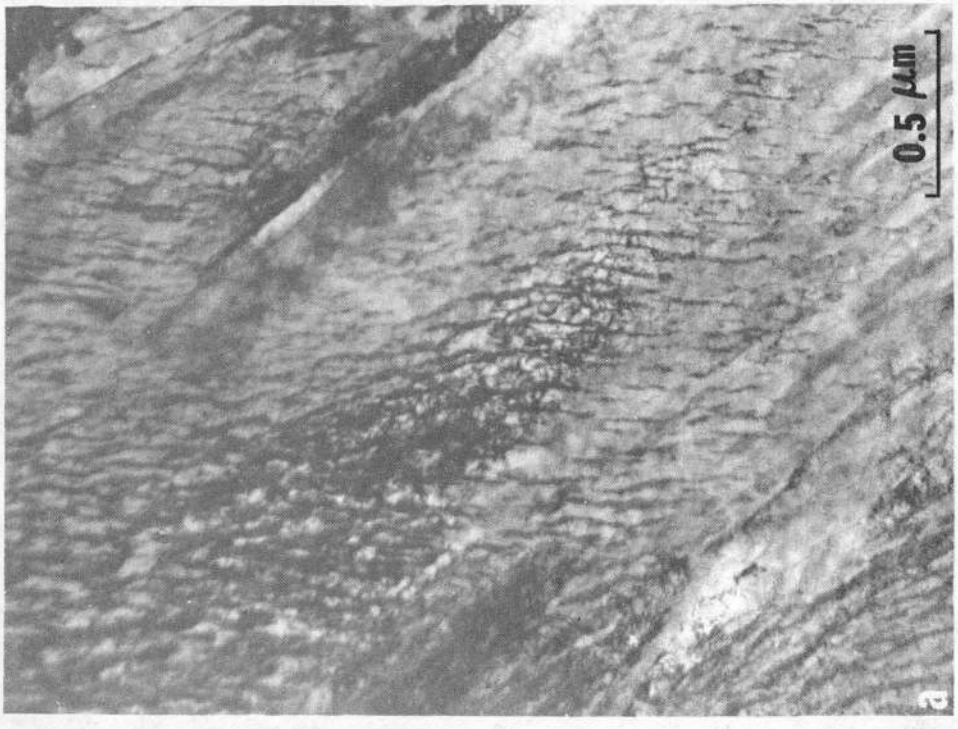

XBB 761-266

FIG. 1

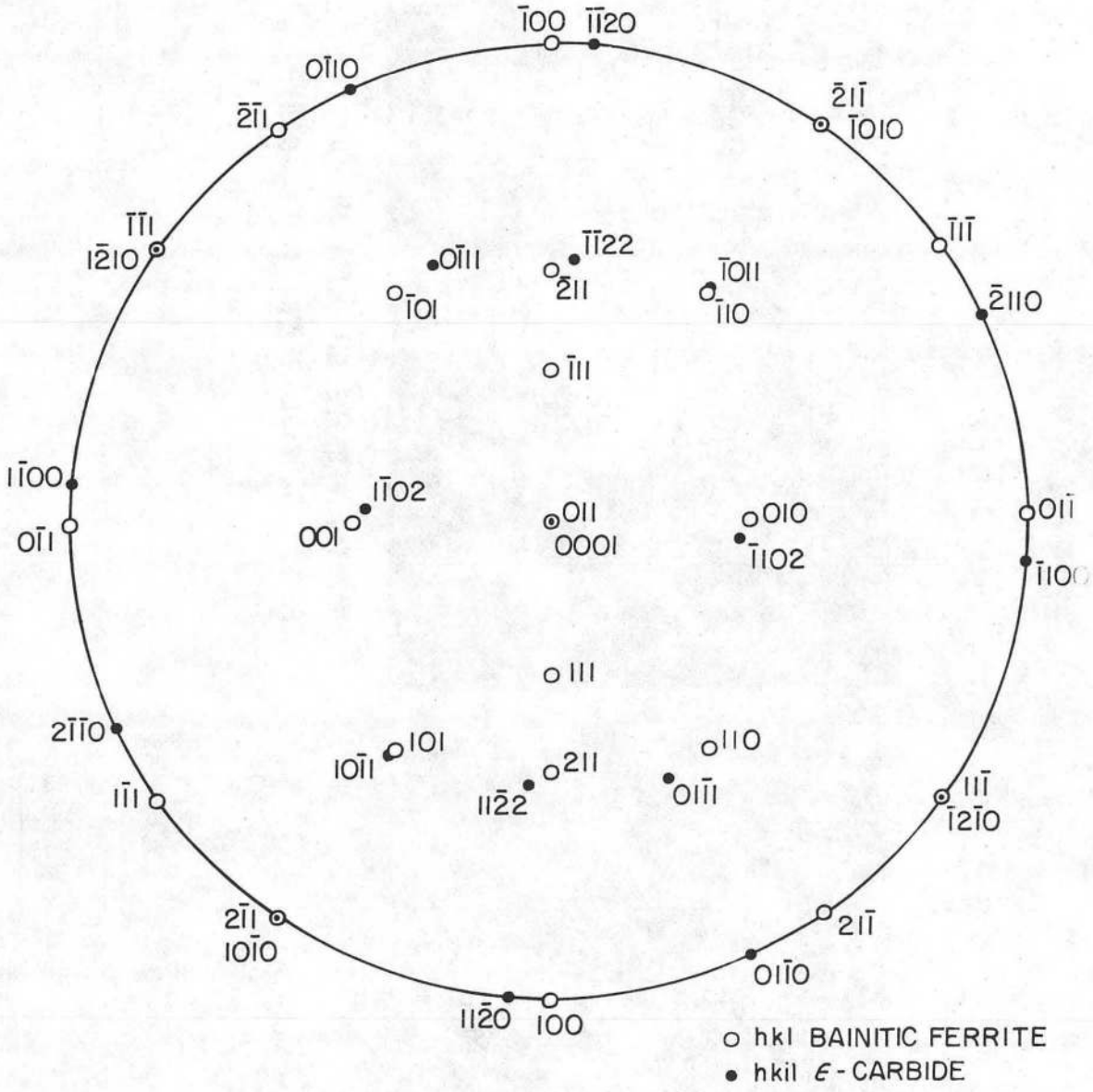

STEREOGRAPHIC PROJECTION REPRESENTING ORIENTATION RELATIONSHIP BETWEEN ϵ CARBIDE AND BAINITIC FERRITE

(0001) ϵ-CARBIDE // (011) FERRITE

(10$\bar{1}$0) ϵ-CARBIDE // ($\bar{2}\bar{1}$1) FERRITE

(10$\bar{1}$1) ϵ-CARBIDE // (101) FERRITE

XBL-735-6152

FIG. 2

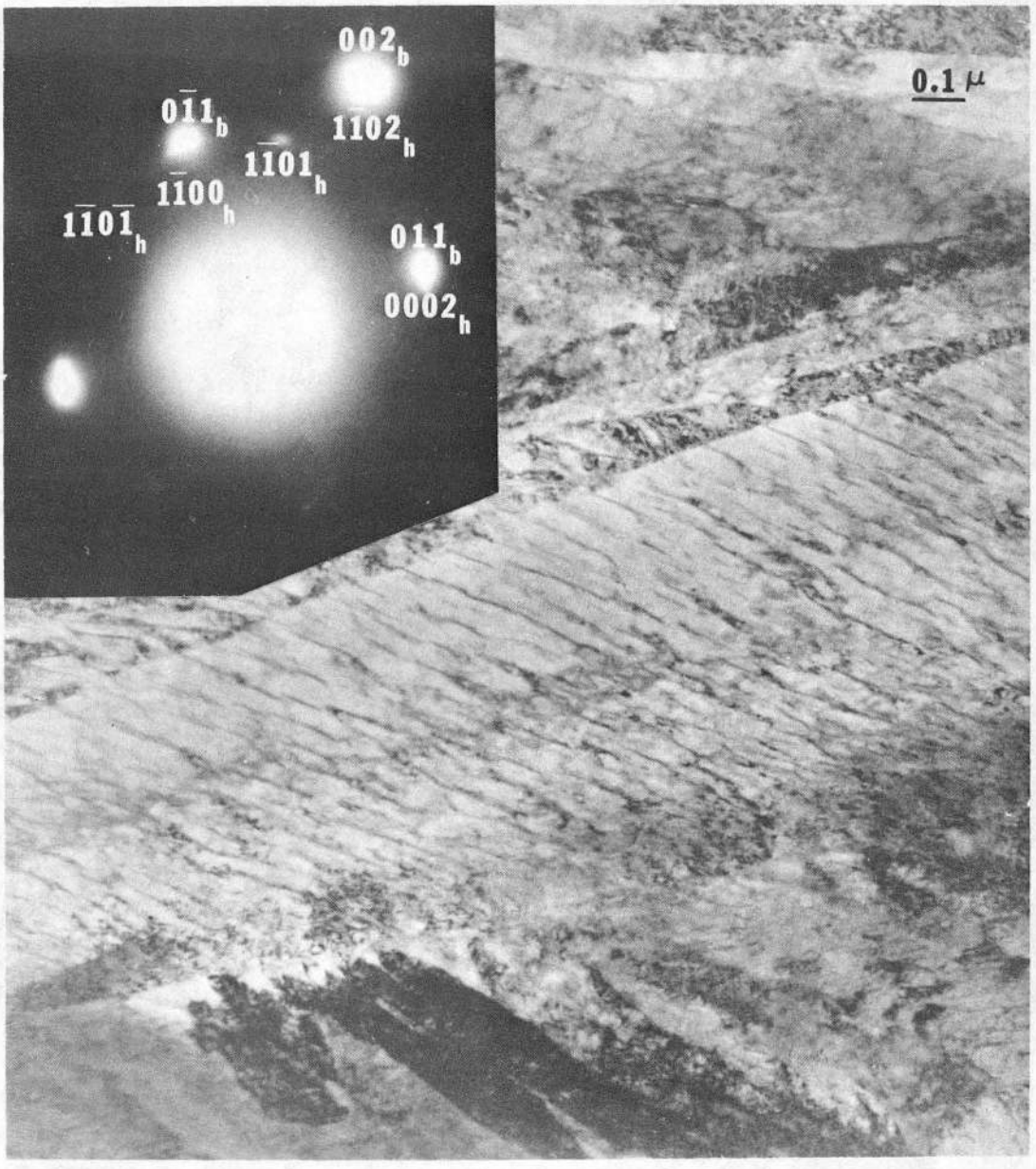

XBB 7212-6112

FIG. 3

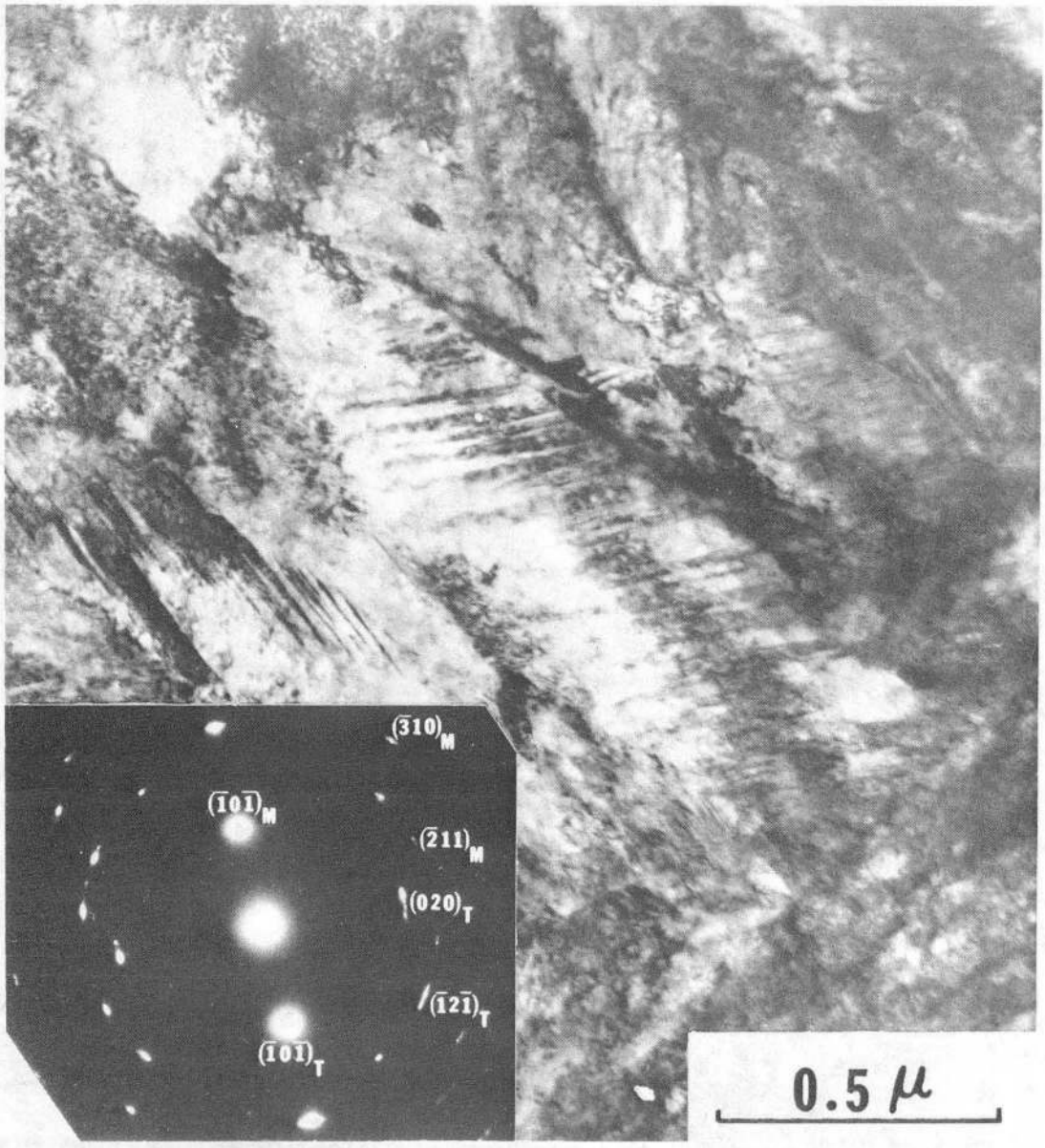

XBB 7510-7493

FIG. 4

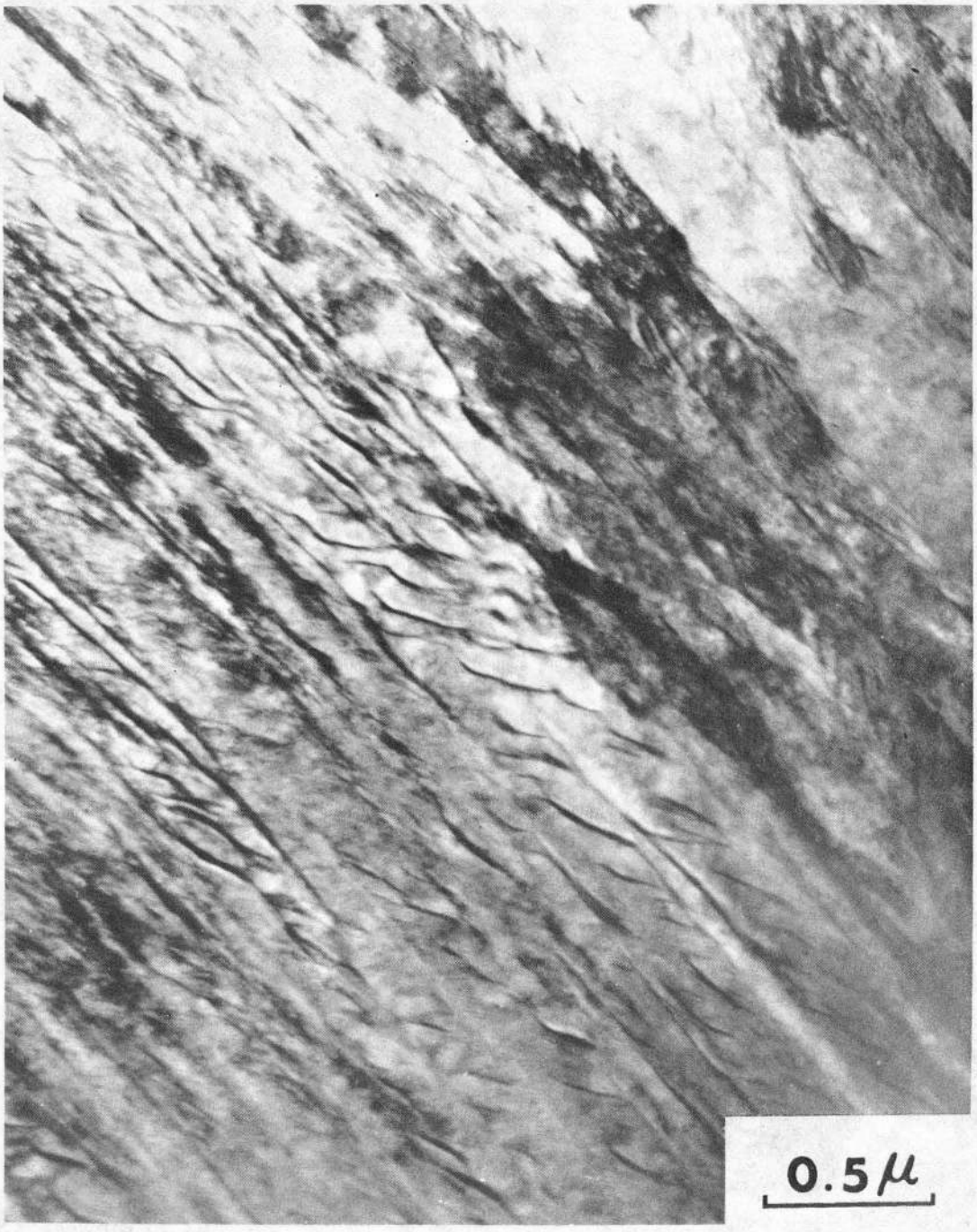

XBB 749-5964

FIG. 5

a

d

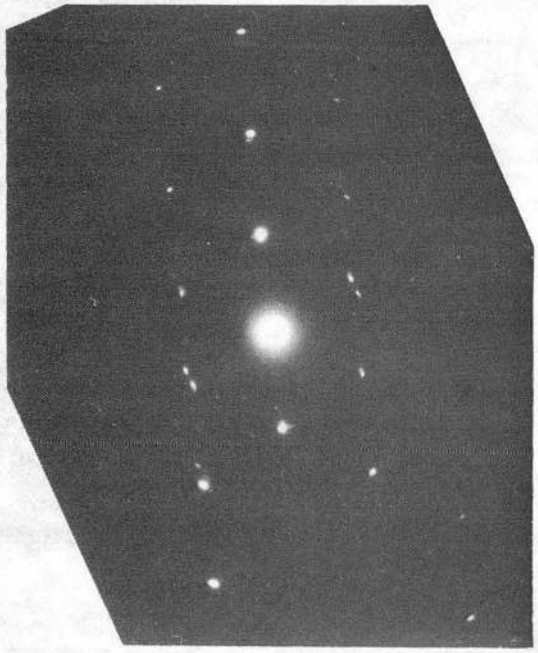

b

XBB 755-3948

FIG. 6 (a) (b) (d)

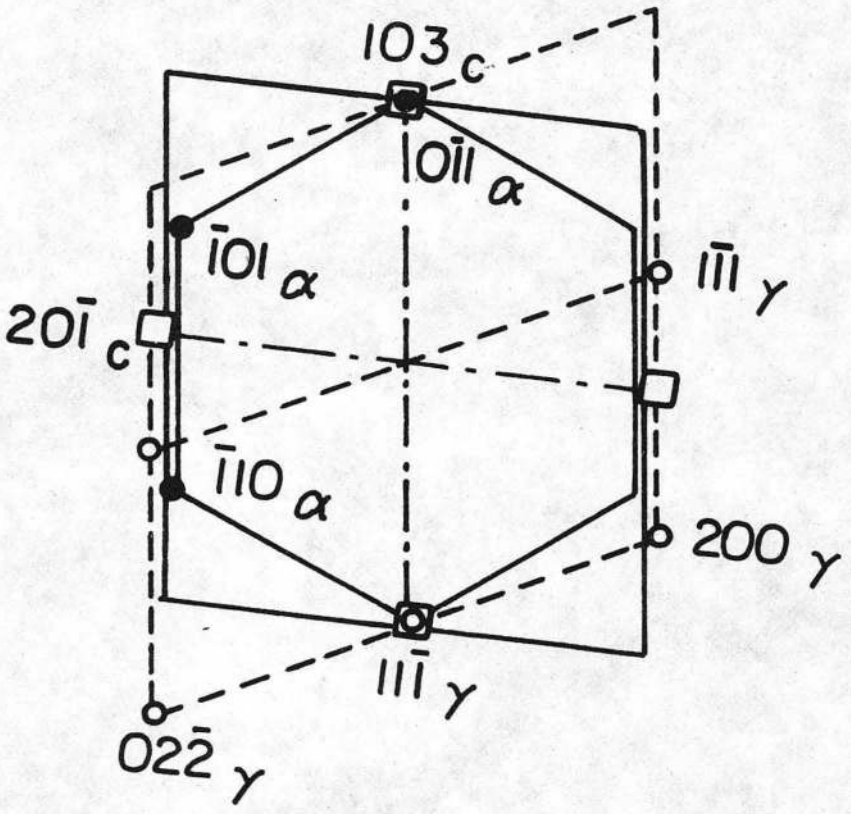

α - ferrite in [111] ——

γ - austenite in [011] – – –

c - cementite [010] —·—

XBL 776-9163

FIG. 6 (c)

XBB 7512-9171

FIG. 6 (e)

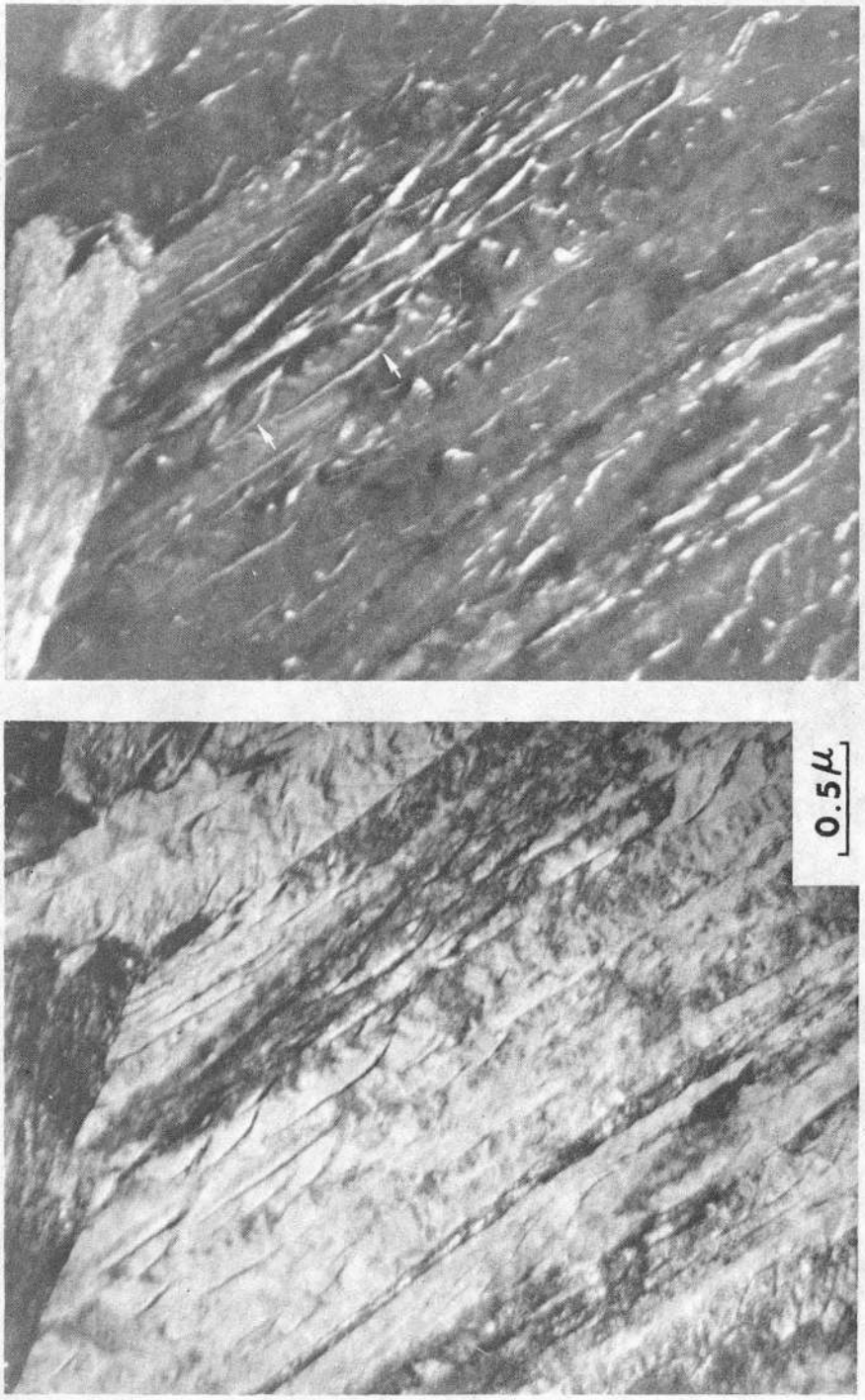

XBB 755-3950

FIG. 7

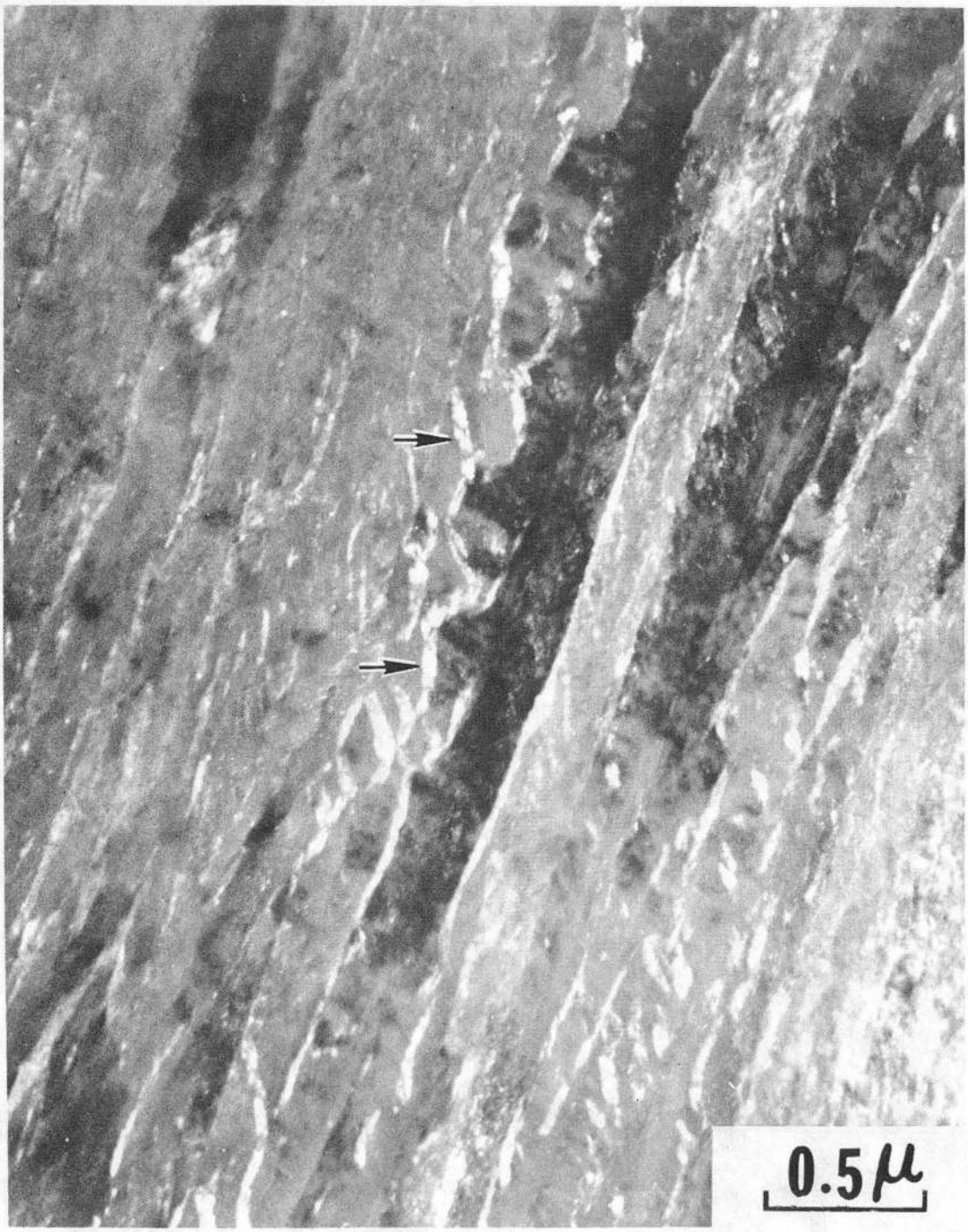

XBB 7510-7914

FIG. 8

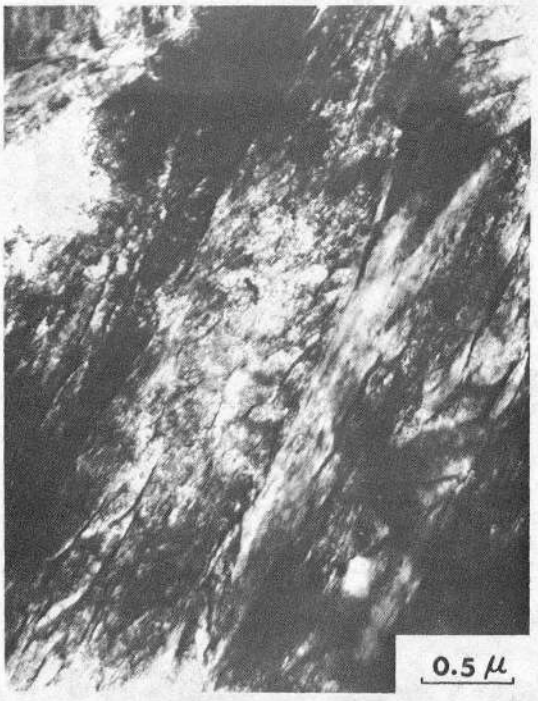

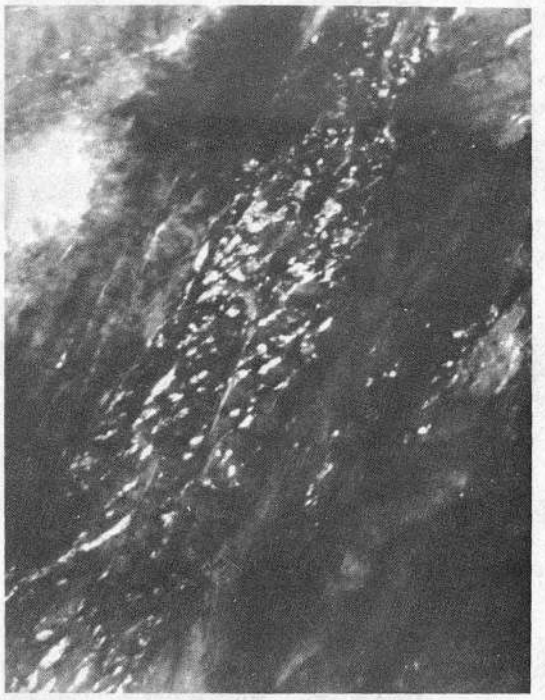

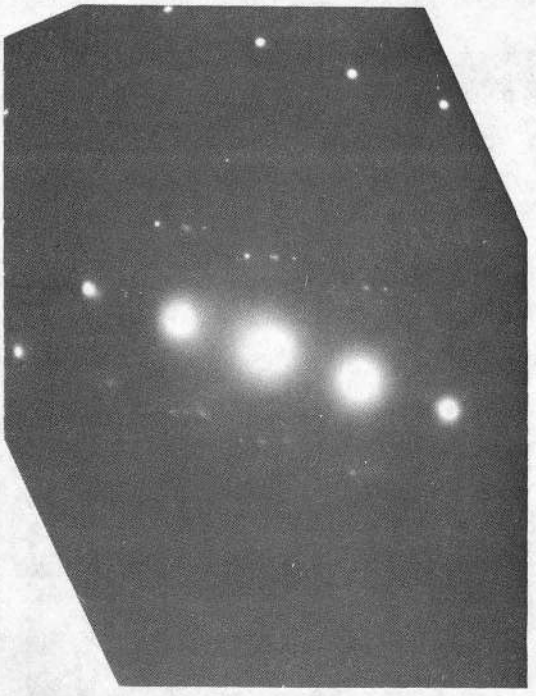

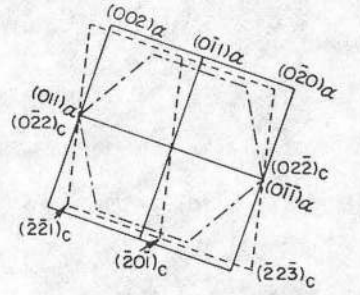

——— FERRITE ORIENTATION $[\bar{1}00]_\alpha$
- - - - - CEMENTITE ORIENTATION $[1\bar{2}\bar{2}]_c$
—·— FERRITE ORIENTATION [111]

XBB 749-5961

FIG. 9

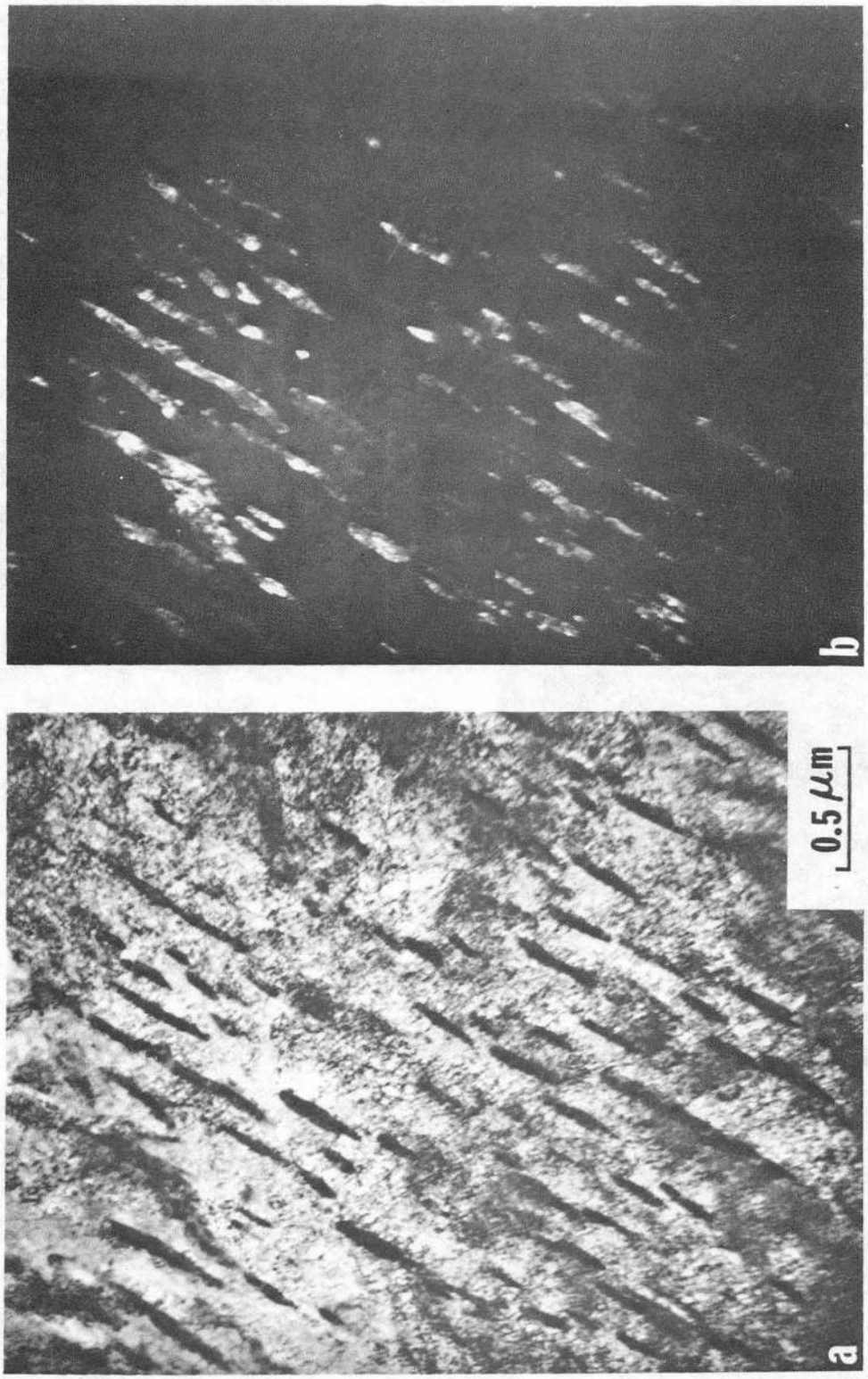

XBB 761-264

FIG. 10

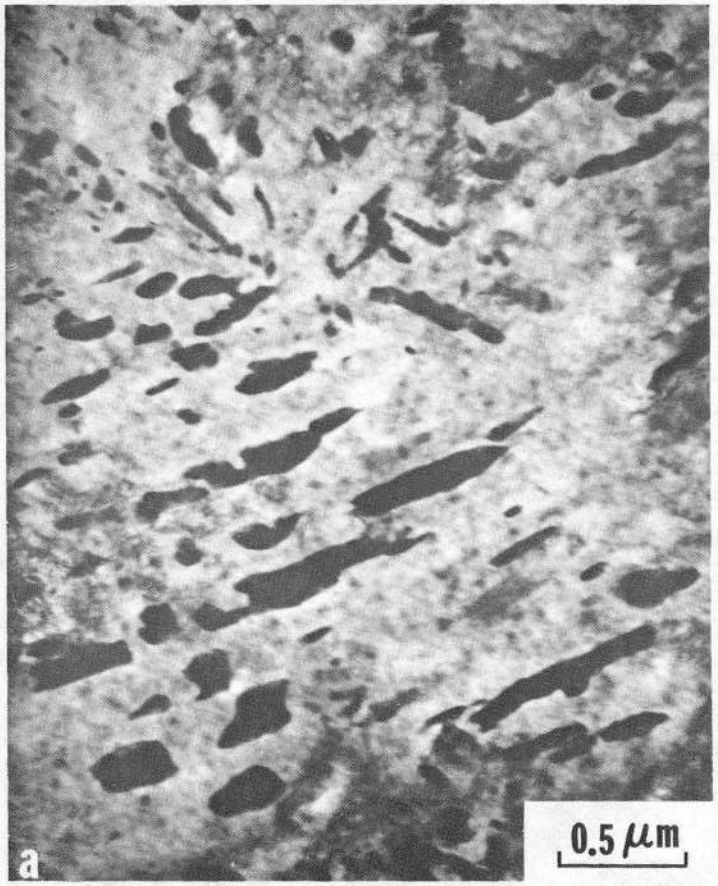

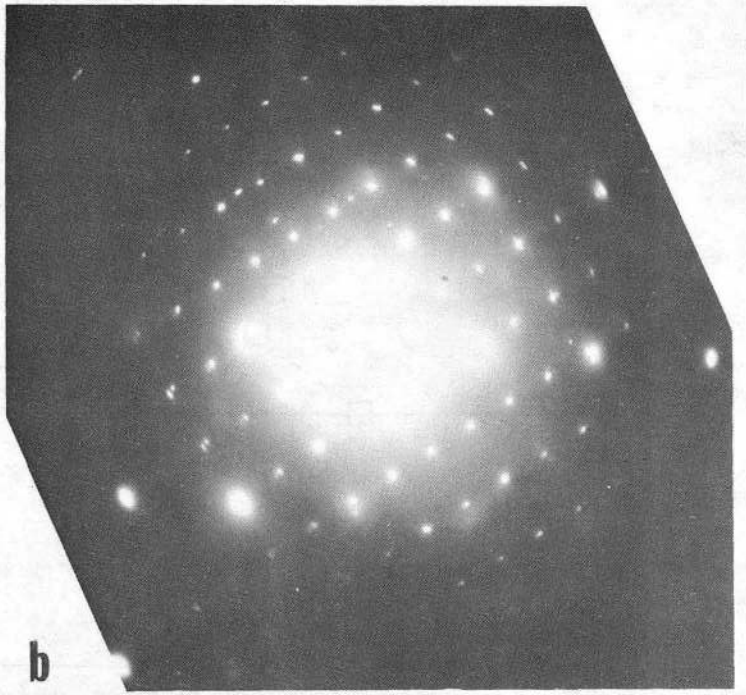

MATRIX ORIENTATION $[\bar{1}10]$
CEMENTITE ORIENTATION $[10\bar{1}]$

XBB 761-265

FIG. 11 (a) (b)

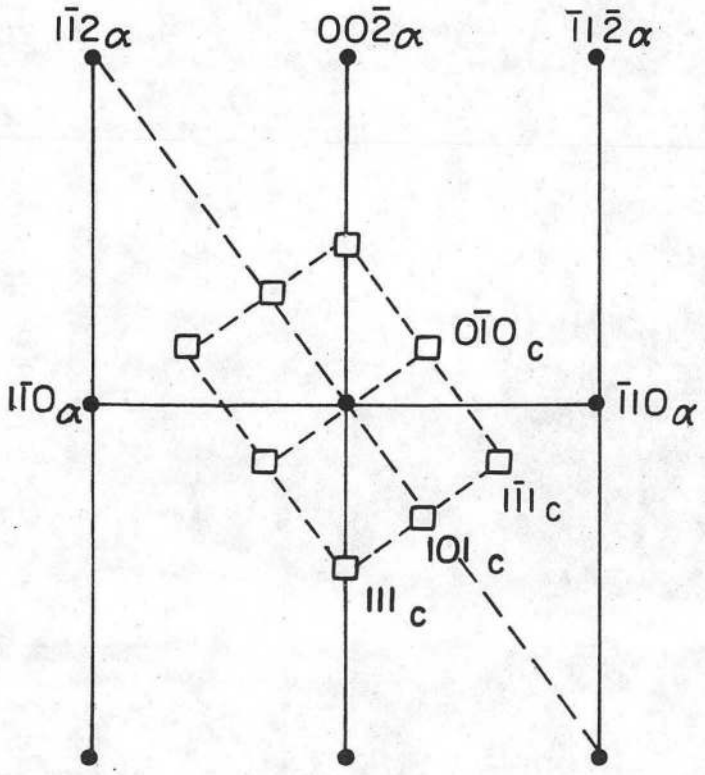

α – ferrite
c – cementite

XBL776-5614

FIG. 11 (c)

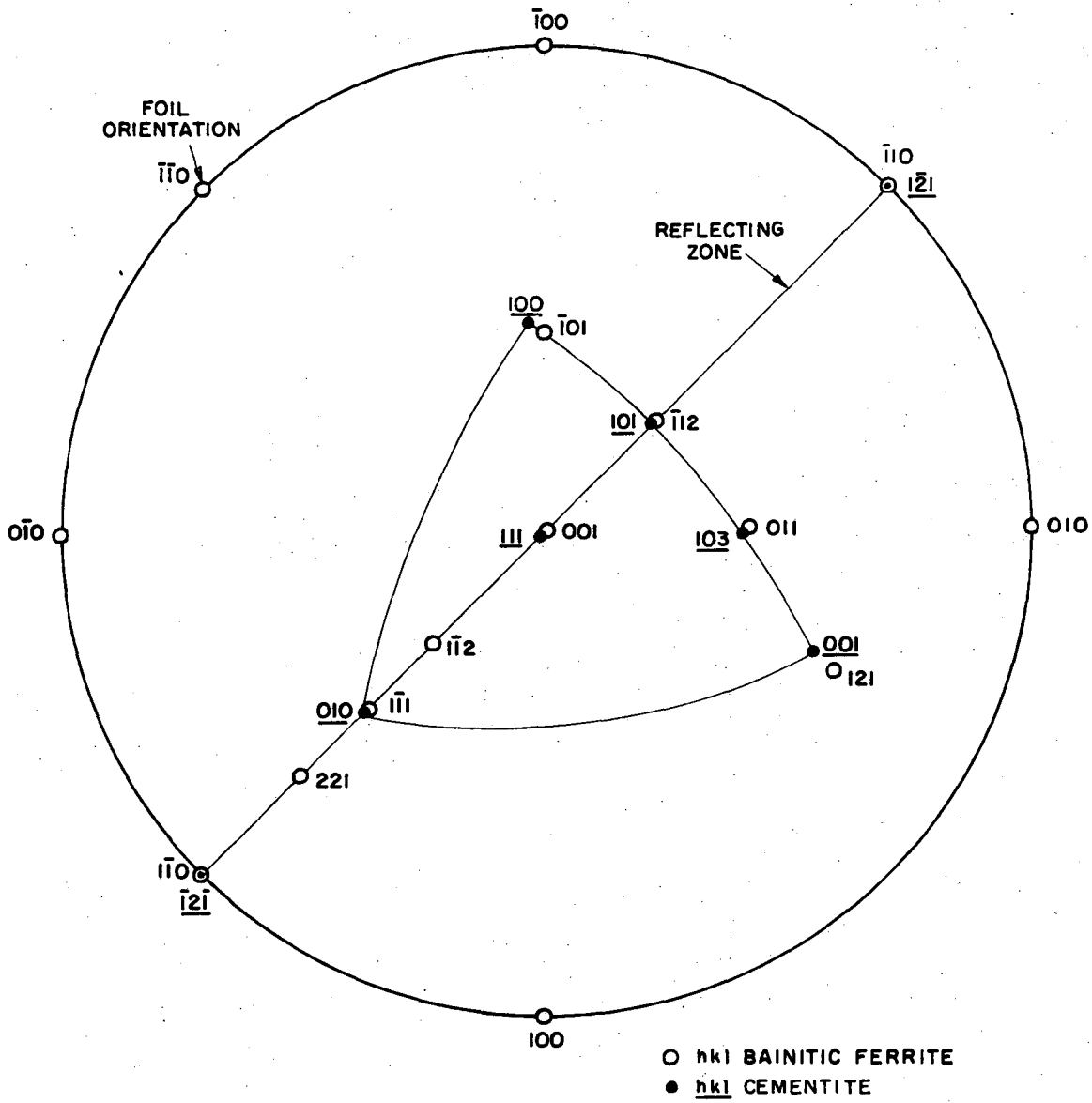

STEREOGRAPHIC PROJECTION REPRESENTING ORIENTATION RELATIONSHIP BETWEEN CEMENTITE AND BAINITIC FERRITE

XBL 735-6187

FIG. 11 (d)

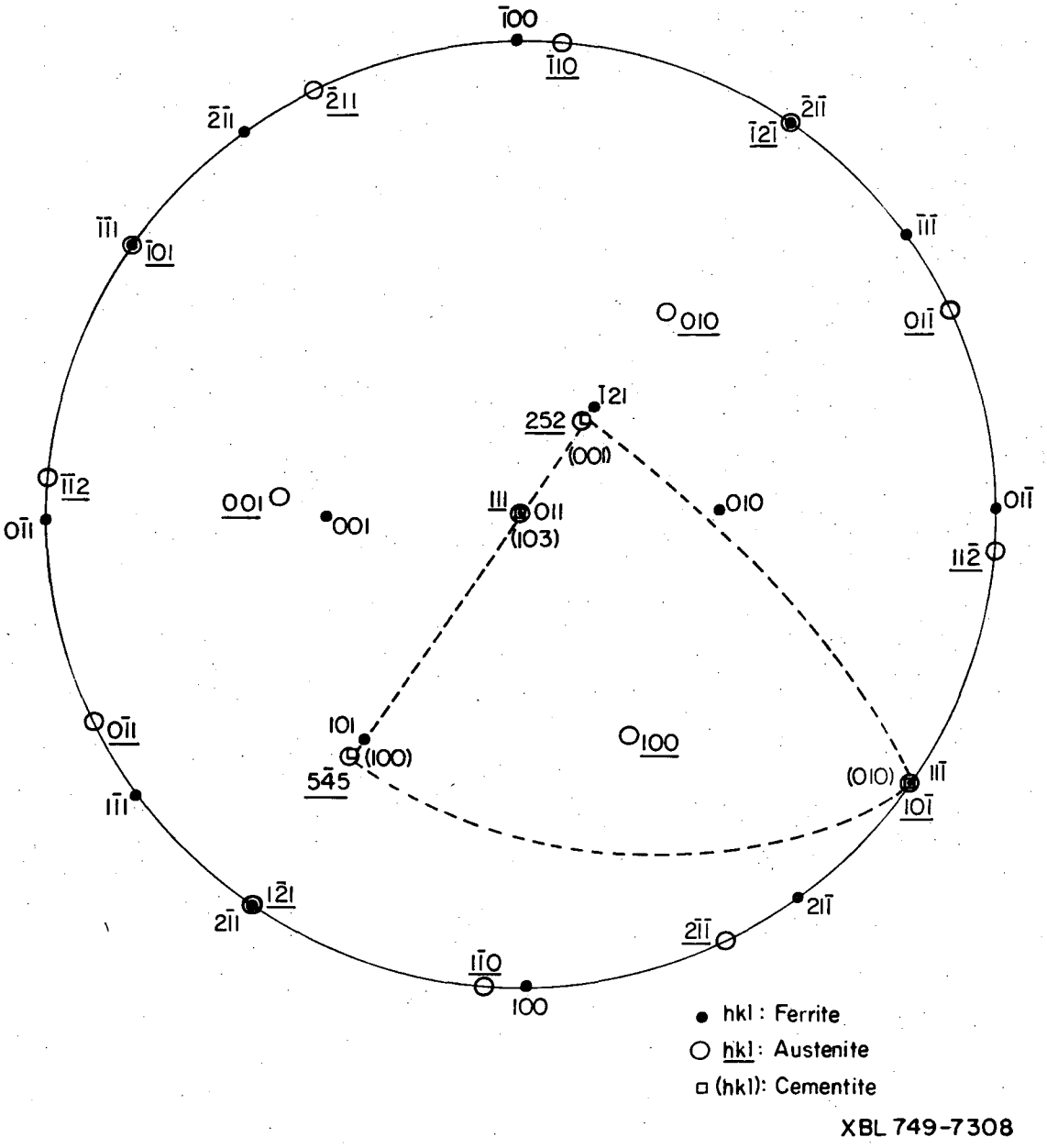
$\bar{1}00$
$\bar{1}10$
$\bar{2}11$
$\bar{2}1\bar{1}$
$\bar{1}2\bar{1}$
$2\bar{1}\bar{1}$
$\bar{1}1\bar{1}$
$\bar{1}01$
$1\bar{1}\bar{1}$
010
$01\bar{1}$
$\bar{1}21$
252
(001)
$\bar{1}\bar{1}2$
001
001
111
011
(103)
010
$01\bar{1}$
$11\bar{2}$
$0\bar{1}1$
101
(100)
$54\bar{5}$
100
(010)
$11\bar{1}$
$10\bar{1}$
$0\bar{1}1$
$1\bar{1}1$
$12\bar{1}$
$2\bar{1}1$
$2\bar{1}\bar{1}$
$21\bar{1}$
$1\bar{1}0$
100
● hkl : Ferrite
○ hkl : Austenite
□ (hkl): Cementite
XBL 749-7308

FIG. 12

TECHNICAL INFORMATION DEPARTMENT
LAWRENCE BERKELEY LABORATORY
UNIVERSITY OF CALIFORNIA
BERKELEY, CALIFORNIA 94720